J. Cent. South Univ. Technol. (2010) 17: 136−141
DOI: 10.1007/s11771−010−0022−6

Springer

Uplift behavior and load transfer mechanism of prestressed high-strength concrete piles

LAI Ying(赖颖), JIN Guo-fang(金国芳)

College of Civil Engineering, Tongji University, Shanghai 200092, China

Abstract: Prestressed high-strength-concrete (PHC) tube-shaped pile is one of the recently used foundations for soft soil. The research on uplift resistance of PHC pile is helpful to the design of pile foundations. A field-scale test program was conducted to study the uplift behavior and load transfer mechanism of PHC piles in soft soil. The pullout load tests were divided into two groups with different diameters, and there were three piles in each group. A detailed discussion of the axial load transfer and pile skin resistance distribution was also included. It is found from the tests that the uplift capacity increases with increasing the diameter of pile. When the diameter of piles increases from 500 to 600 mm, the uplift load is increased by 51.2%. According to the load−displacement (Q−S) curves, all the piles do not reach the ultimate state at the maximum load. The experimental results show that the piles still have uplift bearing capacity.

Key words: prestresed high-strength concrete piles; full-scale test; uplift capacity; load transfer mechanism

1 Introduction

Piles, as an important type of deep foundation, are generally used to transfer axial and horizontal building loads over low strength soil layers or through water body into load bearing strata [1]. The majority of previous studies of the load-deformation behavior of axially loaded piles [2−6] were concerned with the case of compressive loading and were mainly applicable to bored piles. Meanwhile, some researches [7−11] were conducted on the characteristic of driven piles, while relatively little attention was paid to the load−deformation response of driven piles at service uplift load [12−15]. Prestressed high-strength-concrete (PHC) tube-shaped piles belong to a type of the driven piles. They have been widely used in soft soil in recent years partly due to its good properties such as high level in factory production, short curing time, stable quality, high strength and convenient construction. For PHC piles under compressive loading, SHI [16] conducted full-size tests to study the load transfer mechanism including the behavior of skin resistance and toe resistance, and the relationship between the jacking pressure of test piles and the embedded depth was also given; LÜ et al [17] simulated the pile−soil interaction of PHC pile in the soft soil area with finite element method. The calculated distribution trend is in a good agreement with the experimental results. However, PHC piles are required to resist uplift forces in some applications. Therefore, the load−displacement behavior and load transfer mechanism of PHC piles under tensile loading need to be studied. The best approach to understanding the uplift behavior is to conduct full-scale pullout pile load tests.

In this work, full-scaled field tests on six PHC piles were carried out to investigate the uplift capacity and load transfer mechanism of this type of piles. Furthermore, the pile skin resistance distribution along the pile shaft was shown. And the comparison of pile skin resistance in technical code of building pile foundation, geological report and test results was also presented.

2 Experimental

2.1 Pile data and soil condition

The pile load test was carried out in the soft soil area where an underground garage was built. The pile raft foundation was used in the design of underground garage. The lengths of PHC piles were 43 m, and the diameters were 500 and 600 mm, respectively. The pullout load tests were divided into two groups, and three piles in each group. Based on the preliminary design, the standard values of uplift bearing capacity of the PHC piles were 400 kN (group 1, d500 mm, piles 1−3) and 600 kN (group 2, d600 mm, piles 4−6). Field and laboratory tests were carried out for soil characteristics at different depths. The results are summarized in Table 1.

Foundation item: Project(50621062) supported by the National Natural Science Foundation of China
Received date: 2009−02−26; **Accepted date**: 2009−06−23
Corresponding author: LAI Ying, PhD; Tel: +86−13870867881; E-mail: yinglai06@yahoo.com.cn

Table 1 Distribution and characteristics of ground soil

Soil layer No.	Material	Thickness/m	ω/%	e	I_L	I_P	$E_{S_{1-2}}$/MPa	f_{ak}/MPa
1	Plain fill	3.55	30.5	0.947	0.562	13.1	4.09	—
2	Silty clay	0.85	33.9	0.894	0.671	14.3	4.19	90.0
3	Mucky silty clay	8.50	35.4	1.022	1.095	12.0	3.91	80.0
4	Silty soil	7.60	28.7	0.814	0.653	7.2	9.26	160.0
5	Mucky silty clay	10.10	43.0	1.274	1.101	16.3	2.61	60.0
6	Silty clay	8.95	24.6	0.743	0.671	11.7	4.82	180.0
7	Fine sand	2.10	25.4	—	—	—	—	180.0
8	Silty clay	5.05	30.3	0.867	0.731	13.2	4.35	140.0

Note: ω is water content; e is void ratio; I_L is liquidity index; I_P is plasticity index; $E_{S_{1-2}}$ is modulus of compression; f_{ak} is standard value of strata bearing capacity.

2.2 Equipment of steel stress gauges

To study axial load transfer mechanism, 12 water proofed steel stress gauges were attached to the reinforcing cage, which were embedded into the hollow core of PHC pile at depths of 4.0, 12.0, 19.5, 29.5, 38.5 and 42.0 m, respectively. After the reinforcing cage was embedded, concrete was filled in the core of PHC pile. According to the steel stress gauge rating curve and relationship between strain coordinate of concrete and steel, the strain on the pile section can be calculated. Based on the locations of steel stress gauges, the pile was divided into six parts from top to end. The shape of the test pile and positions of stress gauges are shown in Fig.1.

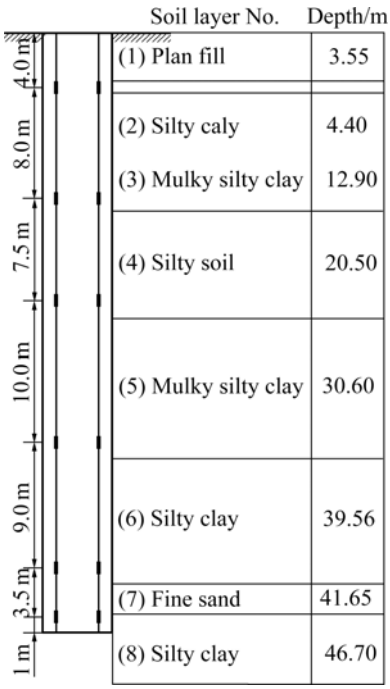

Fig.1 Position of steel stress gauges

2.3 Load test of PHC pile

The pullout load test setup is shown in Fig.2. The pullout load was applied with the help of hydraulic jack placed under the reaction beam. As the load was applied to the PHC pile, the pile top was lifted up slowly. The upward displacement of the pile was measured by two dial gauges with sensitivity of 0.01 mm. Each load increment was maintained for a time interval of 1 h, and for each unload increment the interval was 30 min. The safety factor of 2 was allowed for the ultimate capacity for the design of piles. The design uplift bearing capacity of piles 1−3 was 400 kN, and that for piles 4−6 was 600 kN, so the load applied on the pile top would be more than 800 and 1 200 kN, respectively. The maximum load was 820 kN for piles 1−3, and 1 240 kN for piles 4−6. A summary of the uplift bearing capacity of a single pile, settlement, and rebound ratio is shown in Table 2.

3 Results and discussion

3.1 Relationship between load and settlement for single pile

The load (Q)−settlement (S) curves are shown in Fig.3. The settlement of the pile top increases with increasing uplift load. Due to each load increment, the settlements of piles 1−3 are all less than those of piles 4−6. The average settlement of group 1 is 13.46 mm, and that for group 2 is 20.81 mm. The curves presented in Fig.3 show that the maximum pullout load increases with increasing diameter of the pile. The curves also indicate that, at all stages of loading, the settlement increases with increasing diameter of the pile. The shapes of the curves are similar to those in Fig.3. With the action of the maximum loads 820 and 1 240 kN, the sudden rise point does not appear in the Q−S curves. There is no significant bending in the curves. Then it can be judged that all the piles do not reach the ultimate state because the pile top displacement does not exceed 40 mm, which is the code limit provided by technical code of building pile foundation. It can also be concluded from Fig.3 that there is a discreteness in experimental data. Due to the

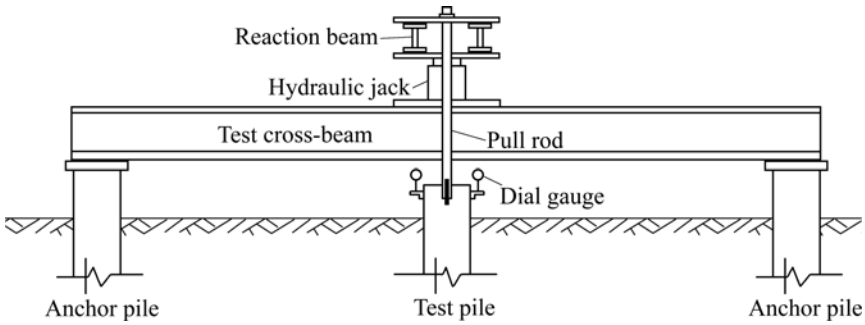

Fig.2 Pullout load test setup

Table 2 Main results of field tests

Pile No.	Diameter/ mm	Maximum load/kN	S_m/ mm	S_r/ mm	R/%
1	500	820	12.64	7.95	37.10
2	500	820	14.02	9.69	35.16
3	500	820	13.73	9.90	27.90
4	600	1 240	24.80	16.80	32.26
5	600	1 240	19.25	13.15	31.69
6	600	1 240	18.37	12.90	29.78

Note: S_m is upward displacement of pile top due to the maximum load; S_r is residual deformation of pile top; R is rebound ratio of pile top.

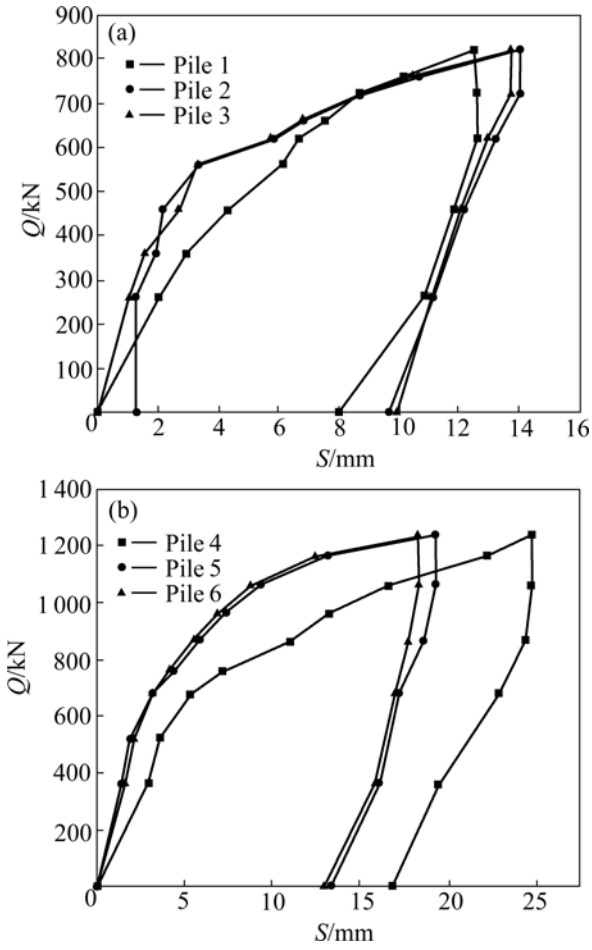

Fig.3 Static load test curves for different piles: (a) Piles 1−3; (b) Piles 4−6

maximum load, the settlements of pile top in group 1 are close to each other, and Q−S curves agree well. However, compared with piles 5 and 6, pile 4 in group 2 has slightly greater settlement due to each load increment. At the maximum load of 1 240 kN, the settlement of pile 4 is 24.80 mm, which is higher than that of piles 5 and 6. The Q−S curves in group 2 are similar in shape, but the Q−S curve of pile 4 does not correspond well with other curves.

3.2 Load transfer along pile shaft

The results of axial load transfer along the six piles' shaft are shown in Fig.4 and Fig.5. The data points were determined from the steel stress gauges reading at each level: Q_i=$E_P\varepsilon_i A_P$ (where Q_i is the axial load of cross section i; E_P is the modulus of pile; ε_i is the strain of cross section i, and A_P is the cross section area of pile). Fig.4 and Fig.5 show that the axial load decreases quickly in the depth range from 0 to 20 m (soil layers 1−4), and the slopes in the figures are relatively large.

For the main soil layer within the range of silty clay, the pile skin resistance is relatively high. In the depth range from 20 to 30 m (soil layer 5), the load decreases slowly and the slopes in the figures get lower due to mucky silty clay in this range, where the pile skin resistance is much lower. Compared with previous range, in the depth range from 30 to 40 m (soil layers 6−8), the load decreases more quickly due to each load increment, and the slope gets higher. This is because there are silty clay and fine sand in this range, where the pile skin resistance is higher than that of mucky silty clay. Due to the maximum load for piles 1−3, soil layer 4 shares 38.4%, 33.9% and 35.5% of the total load, soil layer 5 shares 21.1%, 17.4% and 18.3% of the total load, and soil layers 6−7 share 25.6%, 23.2% and 21.3% of the total load, respectively. Due to the maximum load for piles 4−6, soil layer 4 shares 32.8%, 36.2% and 37.3% of the total load, soil layer 5 shares 13.1%, 15.6% and 16.7% of the total load, and soil layers 6−7 share 20.2%, 24.5% and 25.6% of the total load, respectively. It is obvious in Fig.4 and Fig.5 that at the maximum load the curves do not coincide with the previous load stage

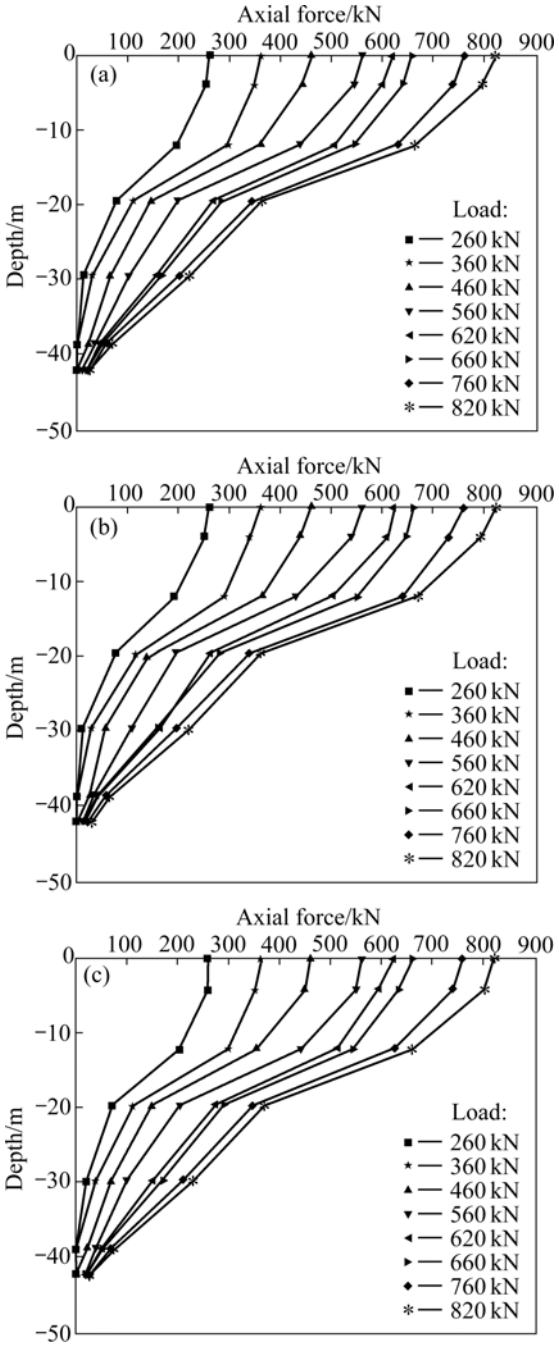

Fig.4 Axial load transfer curves for piles 1−3: (a) Axial force distribution for pile 1; (b) Axial force distribution for pile 2; (c) Axial force distribution for pile 3

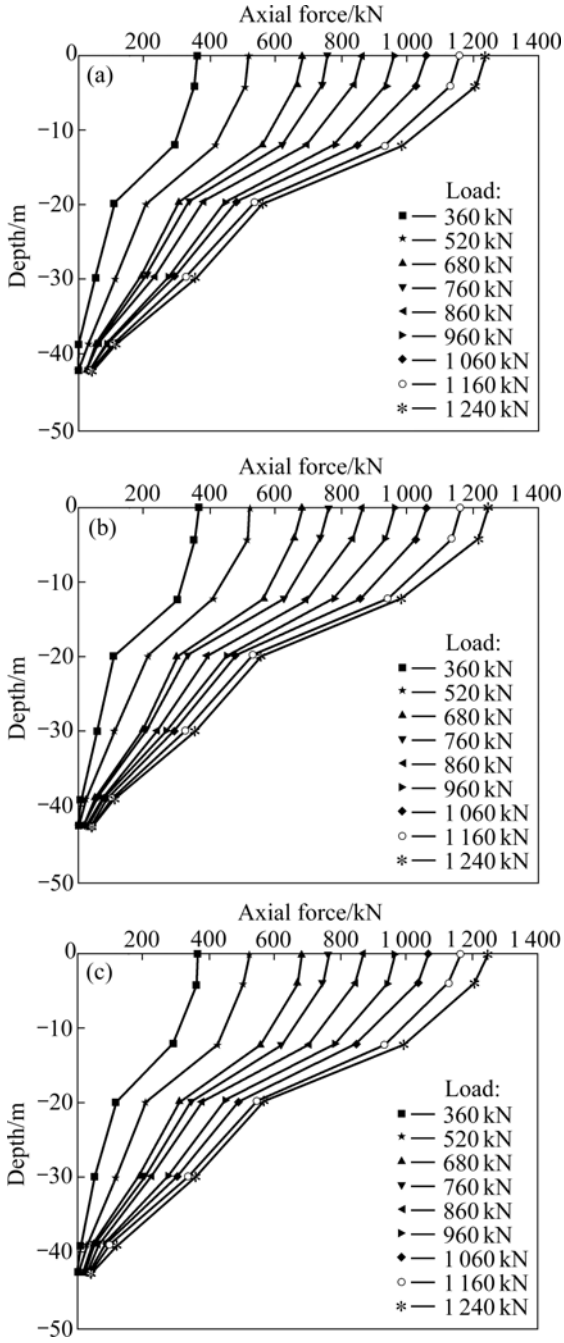

Fig.5 Axial load transfer curves for piles 4−6: (a) Axial force distribution for pile 4; (b) Axial force distribution for pile 5; (c) Axial force distribution for pile 6

curves, which indicates that these PHC piles can bear larger load.

3.3 Pile skin resistance distribution

The average pile skin resistance in each segment can be calculated by axial load distribution measured by the tests. Fig.6 and Fig.7 show the pile skin resistance distribution from pile top to end.

As the load transfers along the pile shaft, the skin resistance exerts gradually from the pile top to pile toe. It is known that the pile skin resistance is related to pile−soil relative displacement, stiffness ratio and soil characteristics [16]. The curves present that pile skin resistance in soil layer 3 is relatively low; the higher value appears in soil layer 4, but in soil layer 5 the pile skin resistance decreases quickly, and in soil layers 6−7 the value increases slightly. The curves of pile skin resistance distribution are approximately “R”-shaped because the bearing capacity of the strata is higher in soil layers 4, 6 and 7 as compared with those of other soil layers.

In Table 3, the pile skin resistances measured in-situ,

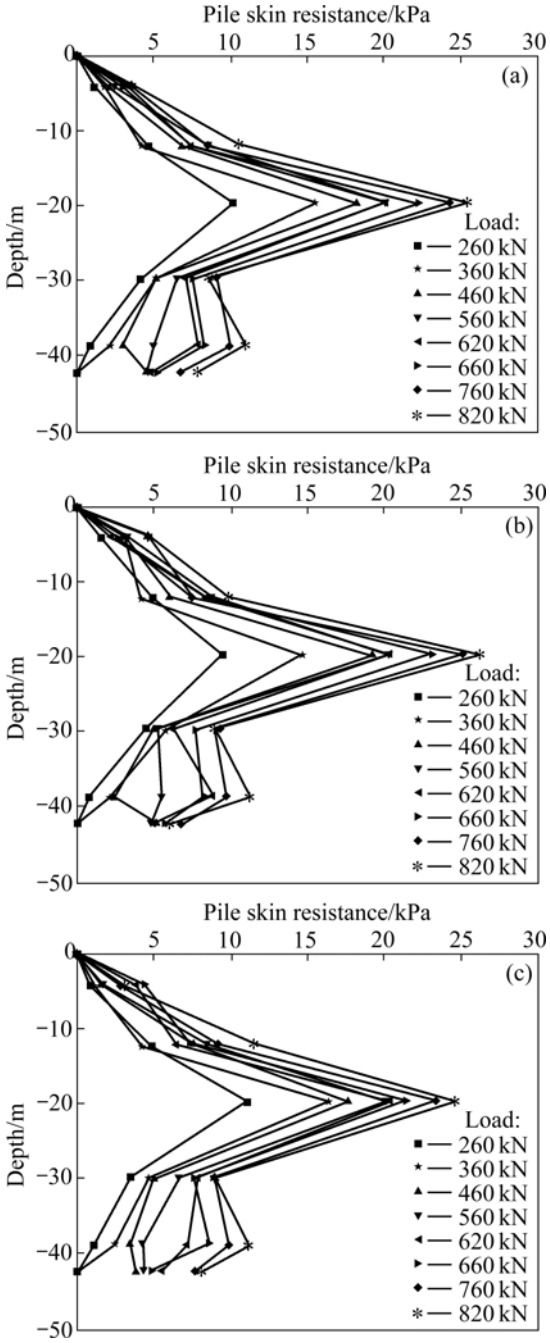

Fig.6 Pile skin resistance distribution for different piles: (a) Pile 1; (b) Pile 2; (c) Pile 3

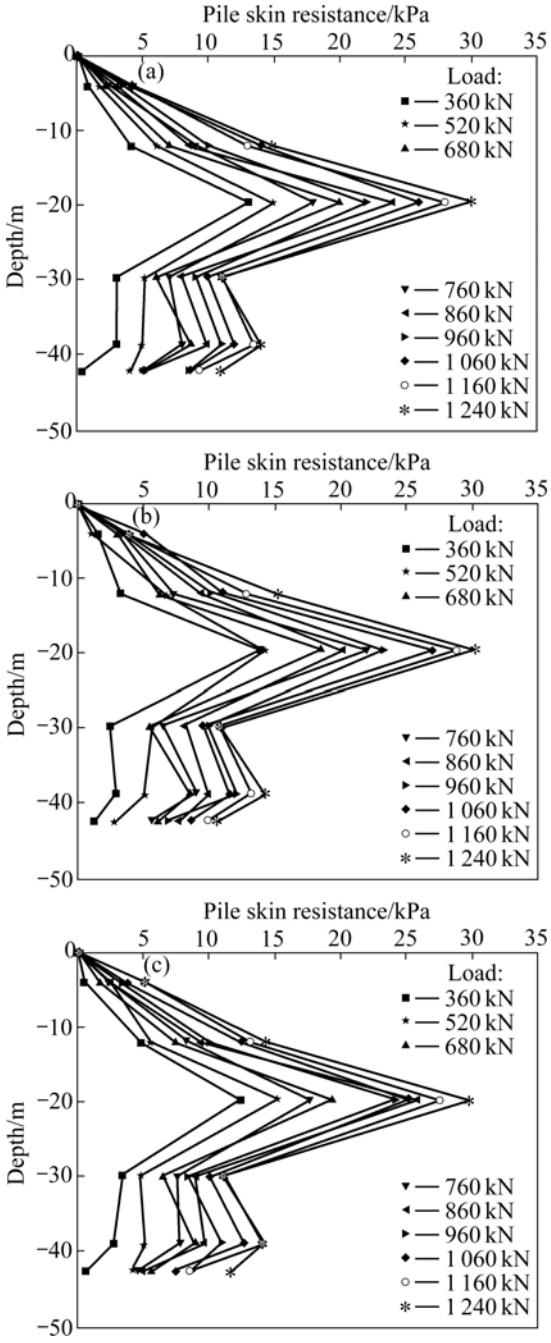

Fig.7 Pile skin resistance distribution for different piles: (a) Pile 4; (b) Pile 5; (c) Pile 6

are compared to those provided by technical code of building pile foundation and geological report. It is clearly that the measured values in soil layers 4−5 are larger than those in geological report, and they do not exceed the ultimate pile skin resistance provided by the technical code. Table 3 indicates that PHC piles have potential uplift capacity in these soil layers. The measured value in soil layers 6−7 is only about a half of that in geological report because soil layers 6−7 are relatively thin, making the pile skin resistance play limited effect.

Table 3 Comparison of pile skin resistance (kPa)

Soil layer No.	JGJ94—94 code	Geological report	Measured value (d500)	Measured value (d600)
4	42−64	20	9−26	12−29
5	20−28	7	9−19	10−20
6	50−66	22	8−12	10−14
7	22−42	27	7−12	8−13

4 Conclusions

(1) An extensive field-test is conducted to study the

behavior of uplift load−settlement, load transfer along the pile and pile skin resistance, respectively. According to the test results, the upward settlement of the pile top increases with increasing uplift load. With the increase of pile diameter, the maximum uplift load and the settlement increase. For the diameter 500 mm of group 1, the uplift loads applied on piles 1−3 are 820 kN and the upward settlements are 12.64, 14.02, and 13.73 mm, respectively. For the diameter 600 mm of group 2, the uplift loads applied on piles 4−6 are 1 240 kN and the upward settlements are 24.80, 19.25, and 18.37 mm, respectively. This is because with the increase of diameter, the surface area of the pile-soil interface increases, causing the increase of uplift capacity.

(2) Due to the uplift load of each increment, the shapes of axial load distribution in the curves are almost "reverse triangle". The axial load decreases quickly in soil layers 4 and 6−8 because there are high pile skin resistances in the corresponding soil layers. The axial load transfer curves under the maximum load stage do not coincide with the curves at previous load stage. This indicates that all the piles can bear larger load. The curves of pile skin resistance distribution are approximately "R"-shaped. The reason is that the bearing capacities of strata in soil layers 4, 6 and 7 are higher than those of others.

(3) The measured pile skin resistance in the tests is higher than that provided by geological report. This shows that the pile skin resistance provided by geological report is relatively conservative.

(4) As all the piles do not reach the ultimate state, the failure mode of PHC piles is not clear yet. Actually, the research on the failure mode is very important for the analysis of bearing capacity and deformation of PHC piles. Therefore, the further research direction is to investigate the influencing factor of the failure mode of PHC piles.

References

[1] KEMPFERT H G, GEBRESELASSIE B. Excavations and foundations in soft soils [M]. Berlin: Springer-Verlag, 2006.

[2] COYLE H M, SULAIMAN I H. Skin friction for steel piles in sand [J]. Soil Mech Foundations Divisions, ASCE, 1967, 93(SM6): 261−278.

[3] GUO W D, RANDOLPH M F. Vertically loaded piles in non-homogenous media [J]. International Journal for Numerical and Analytical Methods in Geomechanics, 1997, 21(8): 507−532.

[4] KIM S, JEONG S, CHO S, PARK I. Shear load transfer characteristics of drilled shafts in weathered rocks [J]. Journal of Geotechnical and Geoenvironmental Engineering, 1999, 125(11): 999−1010.

[5] ZHU Hong, CHANG Ming-fa. Load transfer curves along bored piles considering modulus degradation [J]. Journal of Geotechnical and Geoenvironmental Engineering, 2002, 128(9): 764−774.

[6] ZHU Xiang-rong, FANG Peng-fei, HUANG Hong-mian. Research on super-long pile in soft clay [J]. Chinese Journal of Geotechnical Engineering, 2003, 25(1): 76−79. (in Chinese)

[7] LEHANE B M, WHITE D J. Lateral stress changes and shaft friction for model displacement piles in sand [J]. Canadian Geotechnical Journal, 2005, 42(4): 1039−1052.

[8] ARTHUR K O S, CHARLES W W N. Performance of long-driven H-piles in granitic saprolite [J]. Journal of Geotechnical and Geoenvironmental Engineering, ASCE, 2009, 135(2): 246−258.

[9] MURAD Y A F, HANI H T. Assessment of direct cone penetration test methods for predicting the ultimate capacity of friction driven piles [J]. Journal of Geotechnical and Geoenvironmental Engineering, ASCE, 2004, 130(9): 935−944.

[10] ZHOU Hong-bo, CHEN Zhu-chang. Analysis of effect of different construction methods of piles on the end effect on skin friction of piles [J]. Frontiers of Architecture and Civil Engineering in China, 2007, 1(4): 458−463.

[11] OMER J R, ROBINSON R B, DELPAK R, SHIH J K C. Large-scale pile tests in Mercia mudstone: Data analysis and evaluation of current design methods [J]. Geotechnical and Geological Engineering, 2003, 21(3): 167−200.

[12] RAO A S, PHANIKUMAR B R, BABU R D, SURESH K. Pullout behavior of granular pile-anchors in expensive clay beds in situ [J]. Journal of Geotechnical and Geoenvironmental Engineering, ASCE, 2007, 133(5): 531−538.

[13] ALAWNEH A S. Modeling load−displacement response of driven piles in cohesionless soils under tensile loading [J]. Computers and Geotechnics, 2005, 32: 578−586.

[14] SHANKER K, BASUDHAR P K, PATRA N R. Uplift capacity of single piles: Predictions and performance [J]. Geotechnical and Geological Engineering, 2007, 25(2): 151−161.

[15] GOEL S, PATRA N R. Prediction of load displacement response of single piles under uplift load [J]. Geotechnical and Geological Engineering, 2007, 25(1): 57−64.

[16] SHI Feng. Experimental research on load transfer mechanism of pretensioned high strength spun concrete piles [J]. Chinese Journal of Geotechnical Engineering, 2004, 26(1): 95−99. (in Chinese)

[17] LÜ Wen-tian, WANG Yong-he, LENG Wu-ming. Testing and numerical analysis of load transfer mechanism of PHC pile [J]. Rock and Soil Mechanics, 2006, 27(3): 466−470. (in Chinese)

(Edited by CHEN Wei-ping)